PCCP

PAPER

View Article Online
View Journal | View Issue

Cite this: *Phys. Chem. Chem. Phys.*, 2025, **27**, 13519

Switching of circularly polarised luminescence in perylene-diimide-based chiral liquid crystals induced by electric fields and heating†

Daiya Suzuki,[a] Seika Suzuki,[a] Kosuke Kaneko,[b] Tomonori Hanasaki,[b] Motohiro Shizuma[c] and Yoshitane Imai*[a]

Received 26th April 2025,
Accepted 3rd June 2025

DOI: 10.1039/d5cp01592h

rsc.li/pccp

Two pairs of chiral perylene-based luminescent materials, namely (*R*,*R*)/(*S*,*S*)-*N*,*N*′-bis(1-phenylethyl)-perylene-3,4,9,10-tetracarboxylic diimide [(*R*,*R*)/(*S*,*S*)-**BPP**] and (*R*,*R*)/(*S*,*S*)-*N*,*N*′-bis(1-cyclohexylethyl)-perylene-3,4,9,10-tetracarboxylic diimide [(*R*,*R*)/(*S*,*S*)-**CPDI**], were doped into a nematic liquid crystal with a low phase transition temperature, 4′-hexyl-4-biphenylcarbonitrile. The resultant luminescent chiral nematic liquid crystals (N*-LCs) exhibited a circularly polarised luminescence (CPL) stronger than that of chiral poly(methyl methacrylate)-based luminescent films containing **BPP** and **CPDI**. Both N*-LCs displayed reversible CPL property responses (CPL intensity and CPL sign inversion) upon the application of a direct-current (DC) electric field (due to a chiral nematic phase → nematic phase transition) and heating (due to a chiral nematic phase → isotropic phase transition). Thus, an on–off–on CPL system controlled by DC electric fields and thermal stimuli was constructed based on a transition from a uniformly aligned helical structure to another orientational arrangement. This work provides an effective strategy for the development of functional CPL devices based on CPL control *via* N*-LC exposure to DC electric fields or heat.

Introduction

Liquid crystals (LCs) are versatile soft materials widely used in the fabrication of optoelectronic devices.[1–11] Chiral nematic liquid crystals (N*-LCs) possess a self-organising helical structure and are obtained by adding chiral compounds to nematic liquid crystals (N-LCs). The optical activity of these LC materials is determined by the chirality of the added chiral compounds, which induces the formation of either right- or left-handed helical structures. Therefore, N*-LCs obtained by introducing chiral luminescent materials exhibit circularly polarised luminescence (CPL).[12–16]

Considerable attention has been paid to the development of N*-LCs exhibiting electrically, thermally, and optically controllable CPL to leverage their stimulus response characteristics.[17–21] Such N*-LCs are particularly useful, as their photoluminescence (PL) and CPL properties can be adjusted by applying direct-current (DC) electric fields or heat.[22–32]

Previously, we realised aggregation-enhanced CPL by doping chiral luminescent materials, namely (*R*,*R*)/(*S*,*S*)-*N*,*N*′-bis(1-phenylethyl)perylene-3,4,9,10-tetracarboxylic diimide [(*R*,*R*)/(*S*,*S*)-**BPP**] and (*R*,*R*)/(*S*,S)-*N*,*N*′-bis(1-cyclohexylethyl)perylene-3,4,9,10-tetracarboxylic diimide [(*R*,*R*)/(*S*,*S*)-**CPDI**], into organic polymer films, such as those based on poly(methyl methacrylate) (PMMA).[33–35] These materials were also doped into achiral N-LCs based on 4′-pentyl-4-biphenylcarbonitrile (5CB) to obtain luminescent N*-LCs (N*-LC-5CB/**BPP** and N*-LC-5CB/**CPDI**), which were suitable for further functionalisation and exhibited reversible CPL intensity tuning in response to DC electric field modulation.[36] However, N*-LC-5CB/**CPDI** exhibited CPL sign inversion upon the application of an electric field, whereas no clear inversion was observed for N*-LC-5CB/**BPP**.

Therefore, we aimed to achieve a clear CPL sign inversion through on–off electric field application in **BPP**- and **CPDI**-doped LCs. Additionally, we sought to expand the external stimulus responsiveness of CPL-LCs using heat as the external stimulus and thus develop a reversible CPL switching system. To accomplish these objectives, we used an achiral N-LC based on 4′-hexyl-4-biphenylcarbonitrile (6CB), which has a lower phase transition temperature and longer alkyl chain than the

[a] *Department of Applied Chemistry, Faculty of Science and Engineering Kindai University, 3-4-1 Kowakae Higashi-Osaka, Osaka 577-8502, Japan*
E-mail: y-imai@apch.kindai.ac.jp
[b] *Department of Applied Chemistry, College of Life Sciences Ritsumeikan University, 1-1-1 Nojihigashi Kusatsu, Shiga 525-8577, Japan*
[c] *Morinomiya Center Osaka Research Institute of Industrial Science and Technology, 1-6-50 Morinomiya, Joto-ku, Osaka 536-8553, Japan*

† Electronic supplementary information (ESI) available: ^{1}H NMR spectra of (*R*,*R*)-**BPP**, (*S*,*S*)-**BPP**, (*R*,*R*)-**CPDI**, and (*S*,*S*)-**CPDI**. See DOI: https://doi.org/10.1039/d5cp01592h

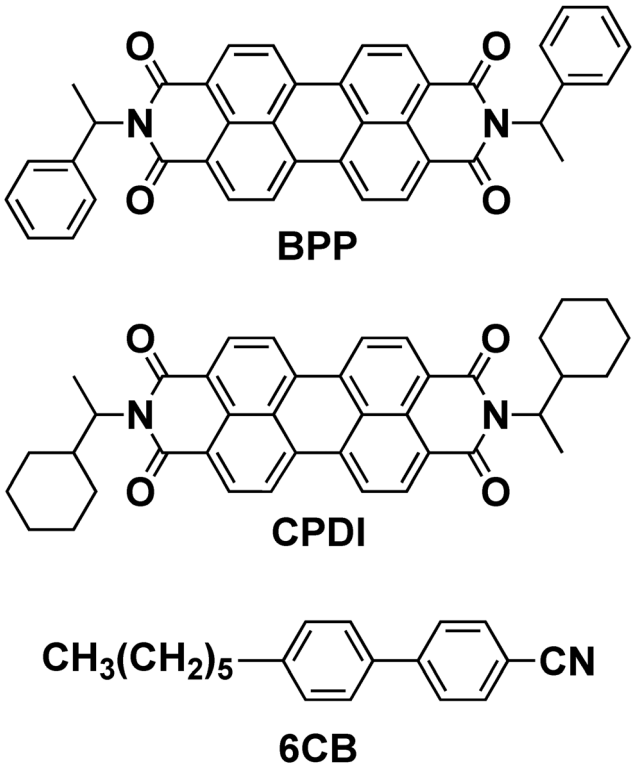

Fig. 1 Chiral perylene-diimide-based luminescent materials (**BPP** and **CPDI**) and the nematic–liquid–crystal compound (6CB) used in this study.

5CB-based achiral N-LC. Luminescent N*-LCs, namely N*-LC-6CB/**BPP** and N*-LC-6CB/**CPDI**, were fabricated by doping (*R,R*)/(*S,S*)-**BPP** and (*R,R*)/(*S,S*)-**CPDI** into the 6CB-based achiral N-LC (Fig. 1). These materials exhibited reversible CPL switching in response to both DC electric fields and heating.

Experimental

General methods

6CB was purchased from Tokyo Chemical Industry Co., Ltd. (Tokyo, Japan). The indium tin oxide (ITO) cell and devices for electric field (KSSZ-10/B107P1NSS05) and temperature (KSSZ-10/D607P1NSS05) control were purchased from EHC Co., Ltd. (Tokyo, Japan). ^{1}H nuclear magnetic resonance (NMR) spectra (JNM-400, JEOL) were recorded at 400 MHz using tetramethylsilane as an internal standard (δ = 0 ppm).

PL and CPL spectroscopy of N*-LC-6CB/BPP and N*-LC-6CB/CPDI

The PL and CPL spectra of LC samples were obtained at 25 and 40 °C using a JASCO CPL-300 spectrofluoropolarimeter (Tokyo, Japan) at a scattering angle of 0°. The samples were excited with unpolarised monochromatic light. For LC analysis, the excitation and emission bandwidths were set to 10 nm. The scan speed and PMT time constant were set to 50 nm min^{-1} and 8 s, respectively, for voltage application and 200 nm min^{-1} and 2 s, respectively, for heating. The LC excitation wavelength was 480 nm. The electric field was applied using an ADCMT 6241A DC voltage current source/monitor. Temperature was controlled using a UNISOKU CoolSpeK CD USP-203CD-B instrument.

Characterisation of LC textures

The optical textures of the LC phases were observed using an Olympus BX53 microscope (Japan) equipped with a high-tech hot stage. The LC materials were inserted into the ITO cell, and the filled cell was observed by polarised optical microscopy (POM) under an applied electric field.

Results and discussion

The chiral luminescent molecules, namely (*R,R*)-**BPP**, (*S,S*)-**BPP**, (*R,R*)-**CPDI**, and (*S,S*)-**CPDI**, were synthesised as described previously[37] and used to fabricate LC devices on conductive ITO glass. (*R,R*)/(*S,S*)-**BPP** and (*R,R*)/(*S,S*)-**CPDI** were doped into N-LC (6CB) at a concentration of 1.0×10^{-2} M to afford N*-LC-6CB/(*R,R*)/(*S,S*)-**BPP** and N*-LC-6CB/(*R,R*)/(*S,S*)-**CPDI**, respectively, which were then placed into conductive ITO glass cells.

The POM images of N*-LC-6CB/(*S,S*)-**BPP** (Fig. 2(a)) and N*-LC-6CB/(*S,S*)-**CPDI** (Fig. 2(b)) acquired at 25 °C revealed a fingerprint texture characteristic of the chiral nematic phase (N*), suggesting that (*S,S*)-**BPP** and (*S,S*)-**CPDI** induced chirality in 6CB. The POM texture of N*-LC-6CB/(*S,S*)-**CPDI** displayed a narrower fingerprint pattern than that of N*-LC-6CB/(*S,S*)-**BPP**, indicating that (*S,S*)-**CPDI** exhibited a stronger chirality and induced a more pronounced helical organisation in the nematic LC.

Therefore, we examined the chiroptical properties of N*-LC-6CB/(*R,R*)/(*S,S*)-**BPP** (Fig. 3(a)) and N*-LC-6CB/(*R,R*)/(*S,S*)-**CPDI** (Fig. 4(a)). N*-LC-6CB/**BPP** and N*-LC-6CB/**CPDI** exhibited high-intensity CPL and PL. In contrast to that observed for PMMA films,[33–35] the CPL of N*-LC-6CB/**BPP** and N*-LC-6CB/**CPDI** in the LC state originated from monomer emission and was characterised by several transition bands (0 → 0, 0 → 1, and 0 → 2) of the perylene unit. The CPL spectra of the (*R,R*) and (*S,S*) LC forms were nearly mirror images of each other.

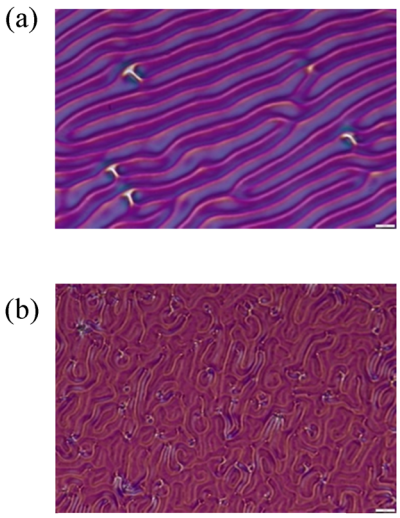

Fig. 2 Polarised optical microscopy (POM) images of (a) N*-LC-6CB/(*S,S*)-**BPP** and (b) N*-LC-6CB/(*S,S*)-**CPDI**.

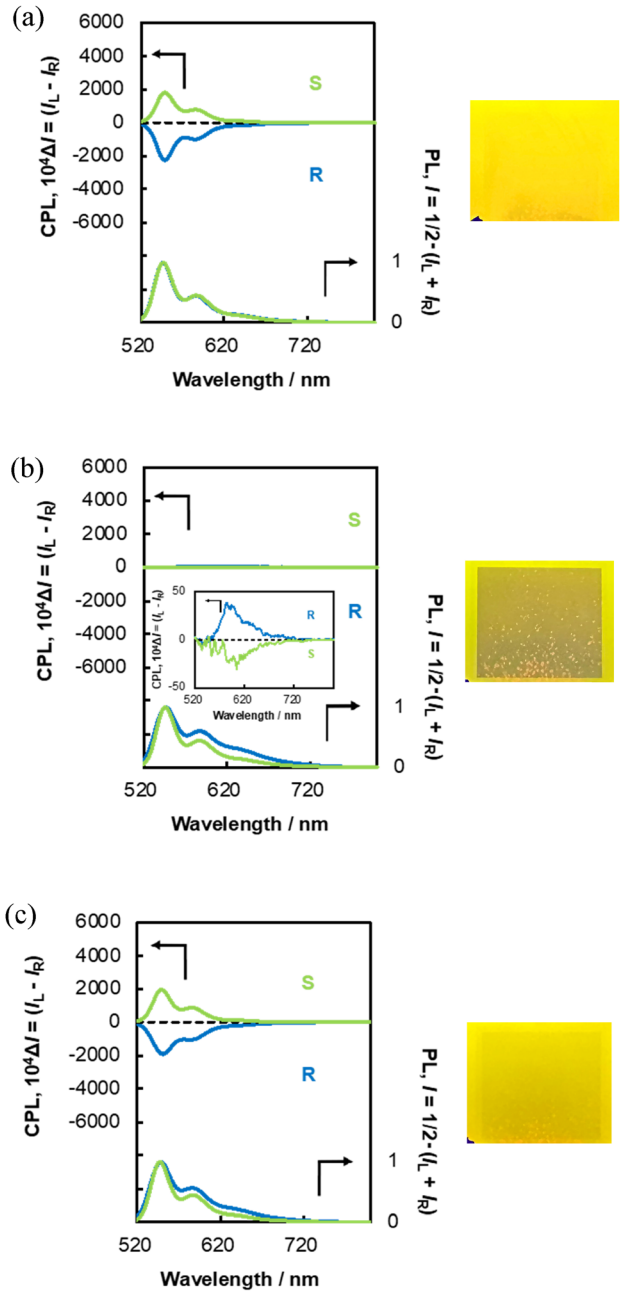

Fig. 3 Circularly polarised luminescence (CPL) (upper chart) and photoluminescence (PL) spectra (lower chart) of N*-LC-6CB/(*R*,*R*)-**BPP** (blue) and N*-LC-6CB/(*S*,*S*)-**BPP** (green) and luminescent images of N*-LC-6CB/(*S*,*S*)-**BPP** (right-hand images) acquired (a) before voltage application at (0 V) (b) at 30 V, and (c) after voltage application at 0 V. The CPL and PL spectra were acquired at an excitation wavelength of 480 nm, while the luminescent images were acquired at an excitation wavelength of 365 nm.

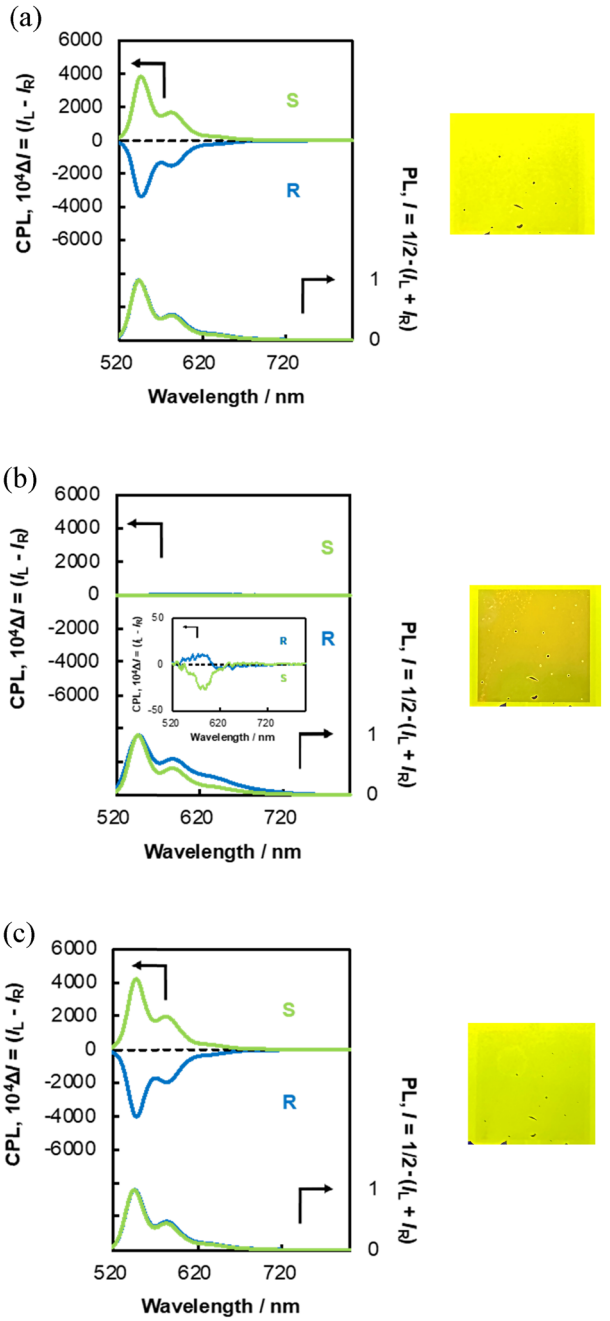

Fig. 4 CPL (upper chart) and PL spectra (lower chart) of N*-LC-6CB/(*R*,*R*)-**CPDI** (blue) and N*-LC-6CB/(*S*,*S*)-**CPDI** (green) and luminescent images of N*-LC-6CB/(*S*,*S*)-**CPDI** (right-hand images) acquired (a) before voltage application at 0 V, (b) at 30 V, and (c) after voltage application at 0 V. The CPL and PL spectra were acquired at an excitation wavelength of 480 nm, while the luminescent images were acquired at an excitation wavelength of 365 nm.

The CPL emission wavelengths (λ_{CPL}) were approximately 550 and 584 nm for N*-LC-6CB/**BPP** and 544 and 583 nm for N*-LC-6CB/**CPDI**. The CPL signals were identical for the chiral S1 state; strong negative signals were observed for N*-LC-6CB/(*R*,*R*)-**BPP** and N*-LC-6CB/(*R*,*R*)-**CPDI**, while positive signals were observed for N*-LC-6CB/(*S*,*S*)-**BPP** and N*-LC-6CB/(*S*,*S*)-**CPDI**. These signal signs were consistent with those observed for N*-LC-5CB/**BPP** and N*-LC-5CB/**CPDI**, indicating that N*-LC-6CB/**BPP** and N*-LC-6CB/**CPDI** possessed a left-handed helical sense in the N* phase. Specifically, (*S*,*S*)-**BPP** and (*S*,*S*)-**CPDI** induced left-handed helical structures, whereas (*R*,*R*)-**BPP** and (*R*,*R*)-**CPDI** induced right-handed helical structures in N-LCs (6CB).[36]

The magnitude of circular polarisation in the excited state is typically defined using the anisotropic dissymmetry factor,

$g_{CPL} = \Delta I/I = 2(I_L - I_R)/(I_L + I_R)$, where I_L and I_R represent the signal intensities for left- and right-hand circular polarisation under excitation with unpolarised light, respectively. The $|g_{CPL}|$ values of N*-LC-6CB/**BPP** and N*-LC-6CB/**CPDI** were approximately 0.19 (550 nm)/0.18 (588 nm) and 0.36 (544 nm)/0.38 (583 nm), respectively. In comparison, the g_{CPL} values of the luminescent **BPP**/PMMA and **CPDI**/PMMA films were substantially lower, with maximum values equalling 2.4×10^{-3} and 7.7×10^{-3}, respectively.

Thus, the g_{CPL} values of N*-LC-6CB/**BPP** and N*-LC-6CB/**CPDI** were approximately 100 times higher than those observed in the PMMA film state and comparable with those in the 5CB LC state. As the transmission wavelength of the liquid-crystalline 6CB falls within the visible-light range, selective reflection can be ignored.[26] The chiral **BPP** and **CPDI** molecules were appropriately fixed by the surrounding 6CB LC molecules, which suppressed the thermal deactivation modes of **BPP** and **CPDI** and resulted in an effective chiral filling arrangement. The very high g_{CPL} in the LC state was attributed to this arrangement, which was similar to that in the 5CB LC state.

The POM images of N*-LC-6CB/**BPP** and N*-LC-6CB/**CPDI** exhibited noticeable changes upon the application of a 30 V DC electric field, indicating that the field induced structural changes in the LC state (Fig. 5). Specifically, the original fingerprint textures changed to a uniformly dark field characteristic of a homeotropic alignment that features rod-like LC molecules oriented perpendicularly to the substrate and results in a minimal birefringence. This alignment is driven by the positive dielectric anisotropy of the LC molecules (6CB), which causes them to align along the direction of the applied electric field. The disappearance of birefringence confirmed that the electric field effectively reoriented the LC molecules into a vertically aligned configuration without the helical structure.

Next, we examined the effect of the applied electric field on the CPL and PL spectra of N*-LC-6CB/**BPP** and N*-LC-6CB/**CPDI**. The CPL intensity of both systems decreased considerably (Fig. 3(b) and 4(b), respectively), although the CPL spectra of the (*R,R*) and (*S,S*) forms remained nearly mirror images of each other. The $|g_{CPL}|$ of N*-LC-6CB/**BPP** at 30 V (5.9×10^{-3} at λ_{CPL} = 585 nm) was notably lower than that at 0 V. Similarly, the $|g_{CPL}|$ of N*-LC-6CB/**CPDI** at 30 V (3.6×10^{-3} at λ_{CPL} = 582 nm) was notably lower than that at 0 V. The CPL sign inversion and red shift observed at 30 V suggested minimal excimer-like CPL emission, although the resolution was reduced because of the decrease in the CPL intensity.[33–36,38]

When the applied field was returned to 0 V, the CPL intensity and $|g_{CPL}|$ of N*-LC-6CB/**BPP** (Fig. 3(c)) and N*-LC-6CB/**CPDI** (Fig. 4(c)) returned to their initial values [approximately 0.20 (550 nm) and 0.19 (584 nm) for N*-LC-6CB/**BPP** and 0.40 (547 nm) and 0.42 (583 nm) for N*-LC-6CB/**CPDI**]. This indicated that CPL from N*-LC-6CB could be switched on and off by the application of a DC electric field, which enabled control over the CPL sign inversion.

This CPL switching was rationalised as follows. In N*-LC-6CB, the **BPP** and **CPDI** molecules were properly aligned along the rod-like 6CB LC molecules, and the planes of the perylene diimide backbones of **BPP** and **CPDI** were therefore nearly parallel albeit twisted relative to each other, similar to the helical structure of N*-LC-6CB. As a result, both **BPP** and **CPDI** exhibited a strong CPL emission. Conversely, the DC electric field applied to **BPP** and **CPDI** induced a high dielectric anisotropy in the LC 6CB molecules, causing them to align perpendicularly to the ITO cell surface. This alignment led to a nematic organisation without a helical structure, resulting in a homeotropic alignment.

The molecular orientation was further corroborated by the POM images captured during the electric field application. Therefore, as the orientation of the LC 6CB molecules changed, **BPP** and **CPDI** also aligned perpendicularly to the ITO cell surface, which resulted in a marked CPL intensity weakening and CPL sign inversion.

Subsequently, we conducted CPL measurements under continuous voltage off-on cycling to investigate the reversibility and durability of the CPL switching behaviour. Both N*-LC-6CB/**BPP** and N*-LC-6CB/**CPDI** exhibited reversible and continuous CPL switching (Fig. 6), *i.e.* their CPL intensity could be regulated continuously and reversibly through the application of a DC electric field.

Subsequently, N*-LC-6CB/**BPP** and N*-LC-6CB/**CPDI** were heated to 40 °C to control the CPL characteristics. The heating of N*-LC-6CB/(*R,R*)-**BPP** and N*-LC-6CB/(*R,R*)-**CPDI** affected their POM images (Fig. 7), which indicated a structural change in the LCs. Upon heating to 40 °C, the N*-LCs transitioned into an isotropic state with random molecular orientations. As a result, a uniformly dark field characteristic of isotropic liquids lacking birefringence was observed under crossed polarisers.

Next, N*-LC-6CB/**BPP** and N*-LC-6CB/**CPDI** were heated to 40 °C, and their CPL and PL spectra were measured. The CPL intensities of N*-LC-6CB/**BPP** (Fig. 8(b)) and N*-LC-6CB/**CPDI** (Fig. 9(b)) decreased markedly upon heating. Under a 30 V DC electric field, clear CPL spectra and sign inversion were

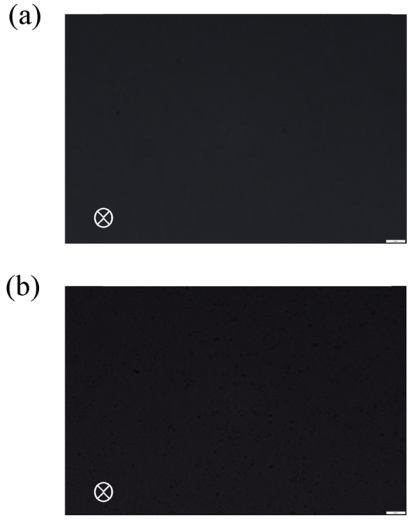

Fig. 5 POM images of (a) N*-LC-6CB/(*S,S*)-**BPP** and (b) N*-LC-6CB/(*S,S*)-**CPDI** acquired upon the application of a direct-current voltage (30 V).

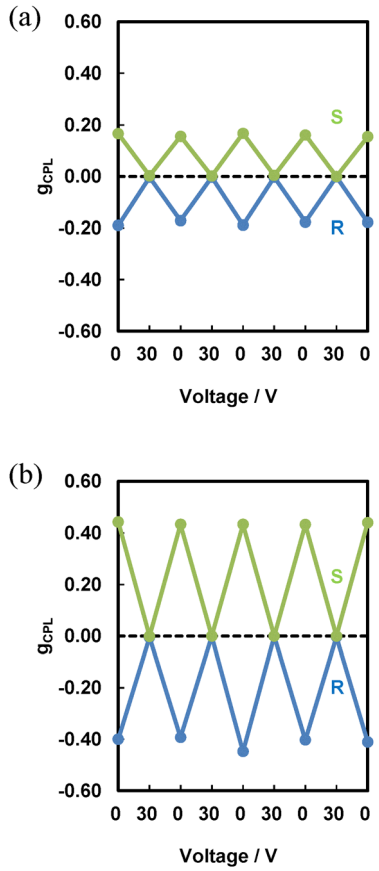

Fig. 6 Evolution of the g_{CPL} of (a) N*-LC-6CB/(*R,R*)-**BPP** (blue) and N*-LC-6CB/(*S,S*)-**BPP** (green) and (b) N*-LC-6CB/(*R,R*)-**CPDI** (blue) and N*-LC-6CB/(*S,S*)-**CPDI** (green) upon switching between 0 and 30 V. An excitation wavelength of 480 nm was used for CPL and PL.

observed; however, at 40 °C, CPL almost disappeared for both N*-LC-6CB/**BPP** and N*-LC-6CB/**CPDI**. Finally, when the temperature was decreased to 25 °C, the CPL intensity and $|g_{CPL}|$ of

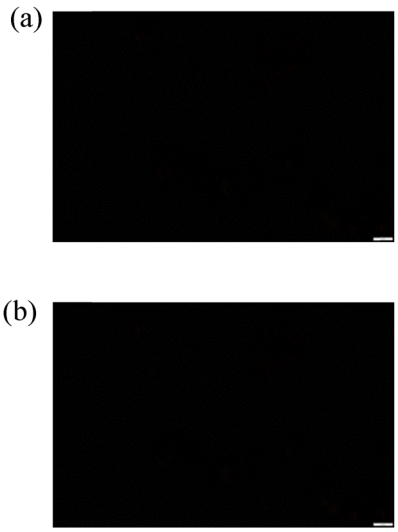

Fig. 7 POM images of (a) N*-LC-6CB/(*S,S*)-**BPP** and (b) N*-LC-6CB/(*S,S*)-**CPDI** upon heating to 40 °C.

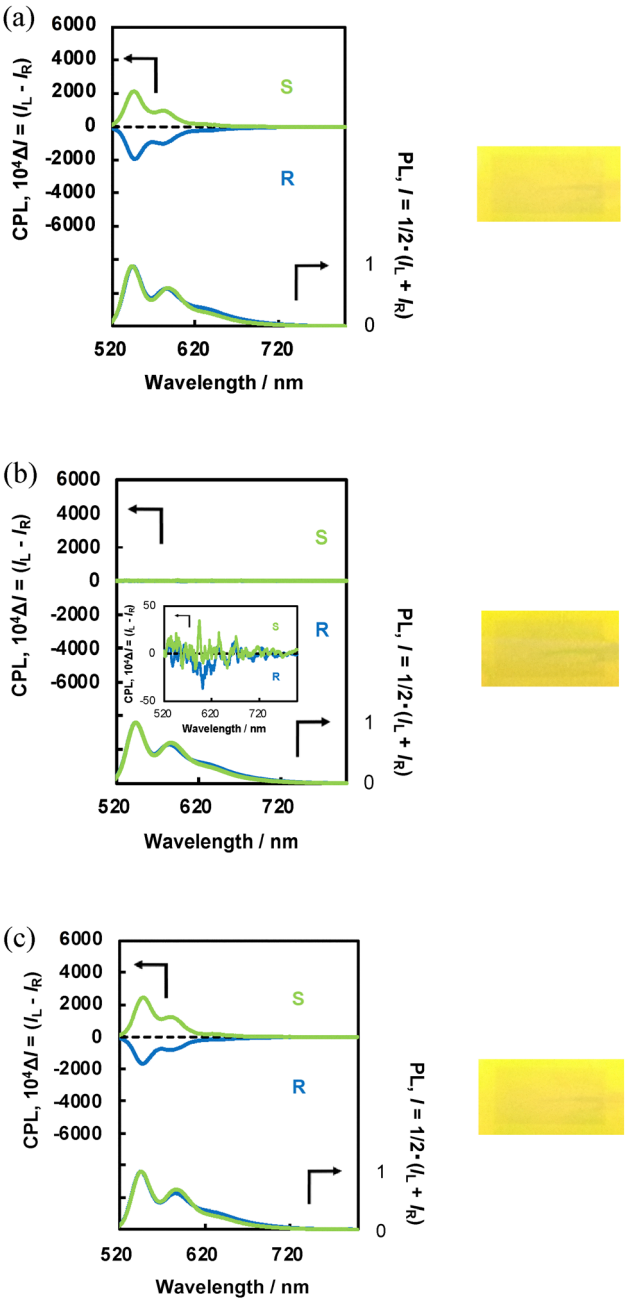

Fig. 8 CPL (upper chart) and PL spectra (lower chart) of the nematic liquid crystal states of N*-LC-6CB/(*R,R*)-**BPP** (blue) and N*-LC-6CB/(*S,S*)-**BPP** (green) and luminescent images of N*-LC-6CB/(*S,S*)-**BPP** (right-hand images) acquired at (a) 25 °C before heating, (b) 40 °C, and (c) 25 °C after heating. The CPL and PL spectra were acquired at an excitation wavelength of 480 nm, while the luminescent images were acquired at an excitation wavelength of 365 nm.

N*-LC-6CB/**BPP** (Fig. 8(c)) and N*-LC-6CB/**CPDI** (Fig. 9(c)) returned to their initial values (see original spectra in Fig. 8(a) and 9(a), respectively): 0.21 (547 nm) and 0.15 (580 nm) for N*-LC-6CB/**BPP** and 0.41 (546 nm) and 0.42 (580 nm) for N*-LC-6CB/**CPDI**. This indicated that the CPL from N*-LC could be turned on and off through temperature adjustments.

The CPL switching due to heating was rationalised as follows. At 25 °C, in the N*-LC-6CB structure, the **BPP** and

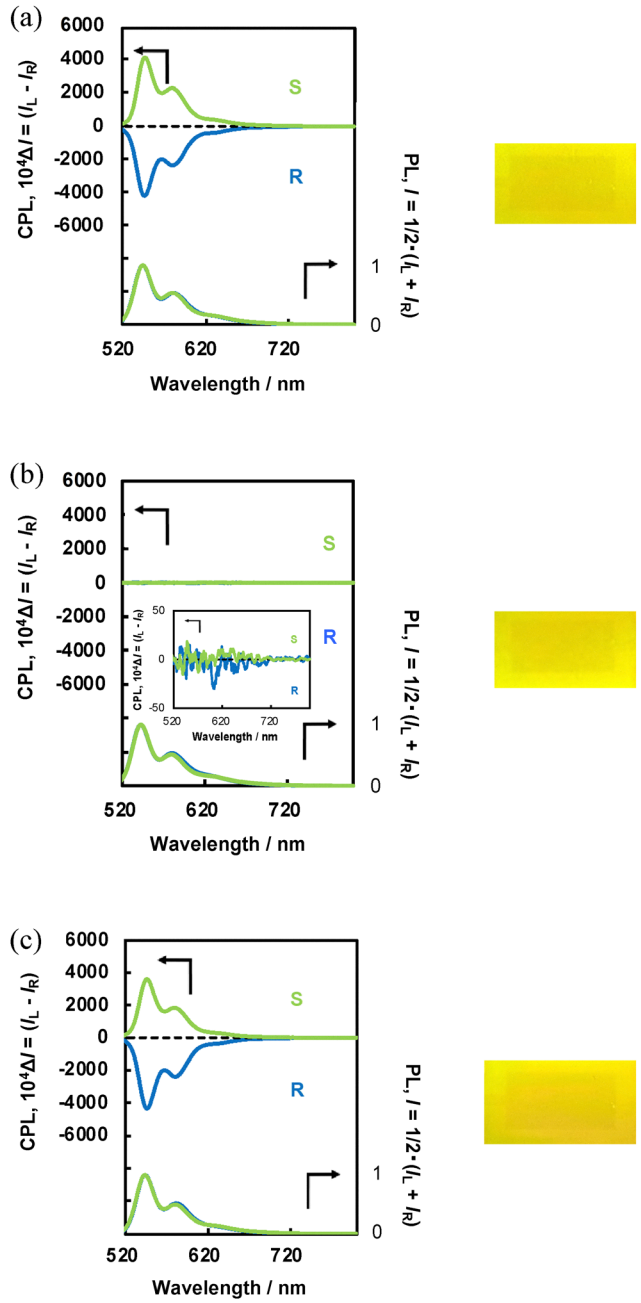

Fig. 9 CPL (upper chart) and PL spectra (lower chart) of the nematic liquid crystal states of N*-LC-6CB/(*R*,*R*)-**CPDI** (blue) and N*-LC-6CB/(*S*,*S*)-**CPDI** (green) and luminescent images of N*-LC-6CB/(*S*,*S*)-**CPDI** (right-hand images) acquired at (a) 25 °C before heating, (b) 40 °C, and (c) 25 °C after heating. The CPL and PL spectra were acquired at an excitation wavelength of 480 nm, while the luminescent images were acquired at an excitation wavelength of 365 nm.

CPDI molecules were twisted relative to each other, similar to the periodic helical structure of N*-LC. However, heating to 40 °C caused a transition from N*-LC to the liquid phase, increasing the number of the degrees of freedom of the **BPP**, **CPDI**, and LC 6CB molecules, which led to reduced molecular orientation and CPL disappearance.

CPL measurements were subsequently performed under thermal cycling conditions (25 °C ↔ 40 °C) to assess the

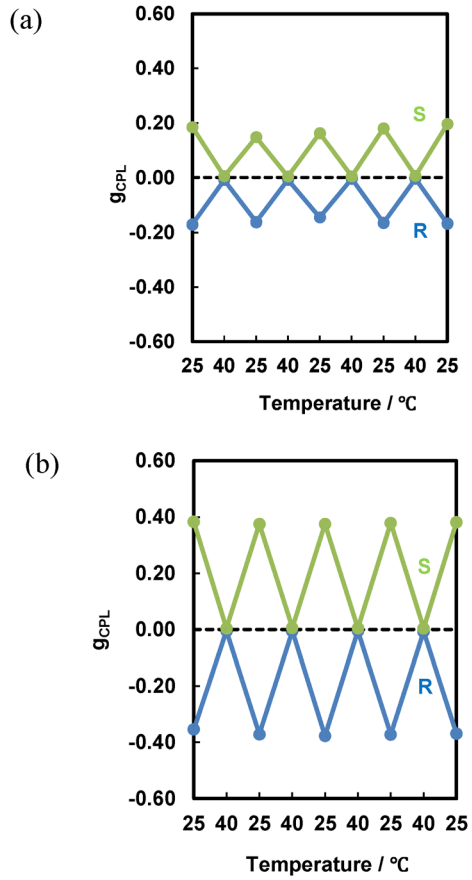

Fig. 10 Evolution of the g_{CPL} of (a) N*-LC-6CB/(*R*,*R*)-**BPP** (blue) and N*-LC-6CB/(*S*,*S*)-**BPP** (green) and (b) N*-LC-6CB/(*R*,*R*)-**CPDI** (blue) and N*-LC-6CB/(*S*,*S*)-**CPDI** (green) upon switching between 25 and 40 °C. An excitation wavelength of 480 nm was used for CPL and PL.

temperature responsiveness of the CPL switching properties. N*-LC-6CB/**BPP** and N*-LC-6CB/**CPDI** maintained reversible and continuous CPL switching performances (Fig. 10), *i.e.* their CPL intensities could be precisely modulated in a continuous and reversible manner *via* temperature variation.

Conclusions

Chiral perylene-diimide-based luminescent materials (**BPP** and **CPDI**) were mixed with 6CB (N-LC) to prepare N*-LC luminescent materials (N*-LC-6CB/**BPP** and N*-LC-6CB/**CPDI**), which exhibited strong CPL emission and anisotropic dissymmetry factors of 0.20 and 0.42, respectively. Reversible CPL switching (CPL intensity and CPL sign inversion) was achieved by adjusting the applied DC electric field, which was attributed to a field-induced structural change from N*-LC to N-LC. In addition, reversible CPL switching was also achieved by applying heat, which was ascribed to a heat-induced structural change from N*-LC to the liquid phase. This study demonstrates that versatile and scalable planar perylene emitters enable CPL switching at different wavelengths with high anisotropic dissymmetry factors. The fabrication of electrically switchable

N*-LC devices will significantly contribute to the advancement of functional CPL materials.

Author contributions

D. Suzuki and S. Suzuki synthesised compounds and performed photophysical measurements. K. Kaneko and T. Hanasaki helped with photoluminescence characterisation. M. Shizuma measured NMR spectra. D. Suzuki wrote the original manuscript. Y. Imai and K. Kaneko revised the manuscript. Y. Imai conceived the project.

Data availability

The data supporting the findings of this study are available in the main article and ESI.†

Conflicts of interest

There are no conflicts to declare.

Acknowledgements

This work was supported by a JST-CREST grant (Grant Number JPMJCR2001), JST-A-STEP grant (Grant Number JPMJTM22D9), Grant-in-Aid for Scientific Research (KAKENHI; Grant Number JP23H02040) from MEXT and JSPS, Iwatani Naoji Foundation Research Grant (Grant Number 23-5012), and IZUMI SCIENCE and TECHNOLOGY Foundation Research Grant (Grant Number 2024-J-062).

References

1 L. M. Blinov and V. G. Chigrinov, *Electrooptic Effects in Liquid Crystal Materials*, Springer, New York, 1996.
2 C. Weder, C. Sarwa, A. Montali, C. Bastiaansen and P. Smith, Incorporation of photoluminescent polarizers into liquid crystal displays, *Science*, 1998, **279**, 835.
3 M. Grell and D. D. C. Bradley, Polarized luminescence from oriented molecular materials, *Adv. Mater.*, 1999, **11**, 895.
4 P. Fischer and F. Hache, Nonlinear optical spectroscopy of chiral molecules, *Chirality*, 2005, **17**, 421.
5 S. Relaix, C. Bourgerette and M. Mitov, Broadband reflective liquid crystalline gels due to the ultraviolet light screening made by the liquid crystal, *Appl. Phys. Lett.*, 2006, **89**, 251907.
6 M. Goh, T. Matsushita, M. Kyotani and K. Akagi, Helical polyacetylenes synthesized in helical sense and pitch controllable chiral nematic liquid crystal with unprecedented temperature dependence, *Macromolecules*, 2007, **40**, 4762.
7 K. Akagi, Helical polyacetylene: Asymmetric polymerization in a chiral liquid-crystal field, *Chem. Rev.*, 2009, **109**, 5354.
8 C. Mowatt, S. M. Morris, M. H. Song, T. D. Wilkinson, R. H. Friend and H. J. Coles, Comparison of the performance of photonic band-edge liquid crystal lasers using different dyes as the gain medium, *J. Appl. Phys.*, 2010, **107**, 043101.
9 T. Geelhaar, K. Griesar and B. Reckmann, 125 years of liquid crystals—A scientific revolution in the home, *Angew. Chem., Int. Ed.*, 2013, **52**, 8798.
10 Y. Chen, J. Lin, W. Yuan, Z. Yu, J. W. Lam and B. Z. Tang, 1-((12-bromododecyl)oxy)-4-((4-(4-pentylcyclohexyl)phenyl)ethynyl)benzene: Liquid crystal with aggregation-induced emission characteristics, *Sci. China: Chem.*, 2013, 56, 1191.
11 J. W. Goodby, P. J. Collings, T. Kato, C. Tschierske, H. Gleeson and P. Raynes, *Handbook of Liquid Crystals*, 2nd edn, Wiley-VCH Press, Weinheim, 2014.
12 D. Zhao, F. Fan, J. Cheng, Y. Zhang, K. S. Wong, V. G. Chigrinov, H. S. Kwok, L. Guo and B. Z. Tang, Light-emitting liquid crystal displays based on an aggregation-induced emission luminogen, *Adv. Opt. Mater.*, 2015, **3**, 199.
13 D. Y. Zhao, H. G. He, X. G. Gu, L. Guo, K. S. Wong, J. W. Y. Lam and B. Z. Tang, Circularly polarized luminescence and a reflective photoluminescent chiral nematic liquid crystal display based on an aggregation-induced emission luminogen, *Adv. Opt. Mater.*, 2016, **4**, 534.
14 Y. H. Shi, P. F. Duan, S. W. Huo, Y. G. Li and M. H. Liu, Endowing perovskite nanocrystals with circularly polarized luminescence, *Adv. Mater.*, 2018, **30**, e1705011.
15 X. J. Li, Q. Li, Y. X. Wang, Y. W. Quan, D. Z. Chen and Y. X. Cheng, Strong aggregation-induced CPL response promoted by chiral emissive nematic liquid crystals (N*-LCs), *Chemistry*, 2018, **24**, 12607.
16 Q. X. Jin, S. X. Chen, Y. T. Sang, H. Q. Guo, S. Z. Dong, J. L. Han, W. J. Chen, X. F. Yang, F. Li and P. F. Duan, Circularly polarized luminescence of achiral open-shell π-radicals, *Chem. Commun.*, 2019, **55**, 6583.
17 N. Y. Ha, Y. Ohtsuka, S. M. Jeong, S. Nishimura, G. Suzaki, Y. Takanishi, K. Ishikawa and H. Takezoe, Fabrication of a simultaneous red-green-blue reflector using single-pitched cholesteric liquid crystals, *Nat. Mater.*, 2008, **7**, 43.
18 R. K. Vijayaraghavan, S. Abraham, H. Akiyama, S. Furumi, N. Tamaoki and S. Das, Photoresponsive glass-forming butadiene-based chiral liquid crystals with circularly polarized photoluminescence, *Adv. Funct. Mater.*, 2008, **18**, 2510.
19 A. Bobrovsky, K. Mochalov, V. Oleinikov, A. Sukhanova, A. Prudnikau, M. Artemyev, V. Shibaev and I. Nabiev, Optically and electrically controlled circularly polarized emission from cholesteric liquid crystal materials doped with semiconductor quantum dots, *Adv. Mater.*, 2012, **24**, 6216.
20 J. Yan, F. Ota, B. A. S. San Jose and K. Akagi, Chiroptical resolution and thermal switching of chirality in conjugated polymer luminescence via selective reflection using a double-layered cell of chiral nematic liquid crystal, *Adv. Funct. Mater.*, 2017, **27**, 1604529.
21 J. Li, H. K. Bisoyi, J. Tian, J. Guo and Q. Li, Optically rewritable transparent liquid crystal displays enabled by light-driven chiral fluorescent molecular switches, *Adv. Mater.*, 2019, **31**, e1807751.
22 T. Hamamoto and M. Funahashi, Circularly polarized light emission from a chiral nematic phenylterthiophene dimer

exhibiting ambipolar carrier transport, *J. Mater. Chem. C*, 2015, **3**, 6891.
23 H. K. Bisoyi and Q. Li, Light-driven liquid crystalline materials: From photo-induced phase transitions and property modulations to applications, *Chem. Rev.*, 2016, **116**, 15089.
24 X. Li, Y. Shen, K. Liu, Y. Quan and Y. Cheng, Recyclable CPL switch regulated by using an applied DC electric field from chiral nematic liquid crystals (N*-LCs), *Mater. Chem. Front.*, 2020, **4**, 2954.
25 L. Wang, A. M. Urbas and Q. Li, Nature-inspired emerging chiral liquid crystal nanostructures: From molecular self-assembly to DNA mesophase and nanocolloids, *Adv. Mater.*, 2020, **32**, e1801335.
26 X. Yang, M. Zhou, Y. Wang and P. Duan, Electric-field-regulated energy transfer in chiral liquid crystals for enhancing upconverted circularly polarized luminescence through steering the photonic bandgap, *Adv. Mater.*, 2020, **32**, e2000820.
27 P. Lu, Y. Chen, Z. Chen, Y. Yuan and H. Zhang, Electric field, temperature and light-triggered triple dynamic circularly polarized luminescence switching in fluorescent cholesteric liquid crystals with a large dissymmetry factor, *J. Mater. Chem. C*, 2021, **9**, 6589.
28 K. Yao, Z. Liu, H. Li, D. Xu, W. H. Zheng, Y. W. Quan and Y. X. Cheng, Reversal of circularly polarized luminescence direction and an ''on-off' switch driven by exchange between UV light irradiation and the applied direct current electric field, *Sci. China: Chem.*, 2022, 65, 1945.
29 X. Zhang, Y. Xu, C. Valenzuela, X. Zhang, L. Wang, W. Feng and Q. Li, Liquid crystal-templated chiral nanomaterials: From chiral plasmonics to circularly polarized luminescence, *Light: Sci. Appl.*, 2022, **11**, 223.
30 J. Liu, Z. P. Song, L. Y. Sun, B. X. Li, Y. Q. Lu and Q. Li, Circularly polarized luminescence in chiral orientationally ordered soft matter systems, *Responsive Mater.*, 2023, **1**, e20230005.
31 Y. Li, Y. Chen, H. Li, C. Liu, L. Li, Y. Quan and Y. Cheng, Achiral dichroic dyes-mediated circularly polarized emission regulated by orientational order parameter through cholesteric liquid crystals, *Angew. Chem., Int. Ed.*, 2023, **62**, e202312159.
32 W. Kang, Y. Tang, X. Meng, S. Lin, X. Zhang, J. Guo and Q. Li, A photo- and thermo-driven azoarene-based circularly polarized luminescence molecular switch in a liquid crystal host, *Angew. Chem., Int. Ed.*, 2023, **62**, e202311486.
33 A. Taniguchi, D. Kaji, N. Hara, R. Murata, S. Akiyama, T. Harada, A. Sudo, H. Nishikawa and Y. Imai, Solid-state AIEnh-circularly polarised luminescence of chiral perylene diimide fluorophores, *RSC Adv.*, 2019, **9**, 1976.
34 K. Watanabe, A. Taniguchi, D. Kaji, N. Hara, T. Hosoya, A. Kanesaka, T. Harada, H. Nishikawa and Y. Imai, Non-classical control of solid-state aggregation-induced enhanced circularly polarized luminescence in chiral perylene diimides, *Tetrahedron*, 2019, **75**, 2944.
35 M. Kitahara, K. Mishima, N. Hara, M. Shizuma, A. Kanesaka, H. Nishikawa and Y. Imai, Circularly polarized luminescence from π-conjugated chiral perylene diimide luminophores: The bay position effect, *Asian J. Org. Chem.*, 2021, **10**, 2969.
36 S. Suzuki, K. Kaneko, T. Hanasaki, M. Shizuma and Y. Imai, Circularly polarized luminescence switching of chiral perylene diimide-doped nematic liquid crystal using DC electric field, *ChemPhotoChem*, 2024, **8**, e202300224.
37 T. Bezrodna, V. Melnyk, V. Vorobjev and G. Puchkovska, Low-temperature photoluminescence of 5CB liquid crystal, *J. Lumin.*, 2010, **130**, 1134.
38 K. Nakabayashi, T. Amako, N. Tajima, M. Fujiki and Y. Imai, Nonclassical dual control of circularly polarized luminescence modes of binaphthyl–pyrene organic fluorophores in fluidic and glassy media, *Chem. Commun.*, 2014, **50**, 13228.

